

An investigation of fMRI time series stationarity during motor sequence learning foot tapping tasks

Othman Muhei-aldin* Jessie VanSwearingen† Helmet Karim‡
Theodore Huppert Patrick J. Sparto Kirk I. Erickson§ Ervin Sejdić

Abstract

Understanding complex brain networks using functional magnetic resonance imaging (fMRI) is of great interest to clinical and scientific communities. To utilize advanced analysis methods such as graph theory for these investigations, the stationarity of fMRI time series needs to be understood as it has important implications on the choice of appropriate approaches for the analysis of complex brain networks. In this paper, we investigated the stationarity of fMRI time series acquired from twelve healthy participants while they performed a motor (foot tapping sequence) learning task. Since prior studies have documented that learning is associated with systematic changes in brain activation, a sequence learning task is an optimal paradigm to assess the degree of non-stationarity in fMRI time-series in clinically relevant brain areas. We predicted that brain regions involved in a “learning network” would demonstrate non-stationarity and may violate assumptions associated with some advanced analysis approaches. Six blocks of learning, and six control blocks of a foot tapping sequence were performed in a fixed order. The reverse arrangement test was utilized to investigate the time series stationarity. Our analysis showed some non-stationary signals with a time varying first moment as a major source of non-stationarity. We also demonstrated a decreased number of non-stationarities in the third block as a result of priming and repetition. The implication of our findings is that future investigations

*Othman Muhei-aldin and Ervin Sejdić are with the Department of Electrical and Computer Engineering, Swanson School of Engineering, University of Pittsburgh, Pittsburgh, PA, 15261, USA. E-mails: oam4@pitt.edu, ese-jdic@ieee.org.

†Jessie VanSwearingen and Patrick J. Sparto are with the Department of Physical Therapy, University of Pittsburgh, Pittsburgh, PA, 15260. E-mails: jessievs@pitt.edu, psparto@pitt.edu.

‡Helmet Karim and Theodore Huppert are with the Department of Radiology, University of Pittsburgh, Pittsburgh, PA, 15261. E-mail: hyppertt@upmc.edu.

§Kirk I. Erickson is with Department of Psychology, University of Pittsburgh, Pittsburgh, PA 15260. E-mails: kiericks@pitt.edu.

analyzing complex brain networks should utilize approaches robust to non-stationarities, as graph-theoretical approaches can be sensitive to non-stationarities present in data.

Keywords: Functional magnetic resonance imaging, time series, stationarity, reverse arrangement test, foot tapping.

1 Introduction

Investigating brain networks involved in complex cognitive, affective, or motor tasks are of great interest from scientific and clinical perspectives. To define brain networks, researchers have used various experimental modalities such as structural and functional magnetic resonance imaging (MRI) [1], [2], [3], positron emission tomography (PET) [3], diffusion tensor imaging [1], magnetoencephalography [4], and electroencephalography [5]. The most common modality is fMRI, first shown in 1992 to be useful for exploring functional brain activity [6]. Since then, fMRI has been widely used to study brain networks involved in a variety of psychological and motor behaviors using several signal processing approaches [1], [2], [3], [4], [5]. MRI has enabled us to understand the brain macroscopic organization by enabling us to study the structural and functional networks [7]. The use of fMRI to study brain activation patterns has several advantages over other methods such as PET, which requires radioactive ligands to be injected into the participants. fMRI: (1) is considered a non-invasive technology for acquiring brain images, (2) can be used to examine task performance in less time, acquiring scan images more rapidly than the PET, and (3) the scans have high spatial resolution [8]. The blood oxygenation and flow is the fundamental basis for fMRI. Thus the brain activation signal increases around the area of blood vessels and brain tissues with higher blood oxygenation levels and blood flow [3], [9], [10]; the more activated brain regions have higher blood flow and blood oxygenation than non-active regions [3], [9], [10]. Hence, the measured signal by fMRI depends on the change of oxygenation which is referred to as the Blood Oxygen Level Dependent (BOLD) signal [9], [11].

The vast majority of recent contributions on complex brain networks are based largely on graph theory analysis [12]. The graph theoretical analysis of MRI data has been widely used to understand both normal brain networks and dysfunctional brain networks resulting from pathologies such as Alzheimer's disease [7], [13], [14], [15], schizophrenia [7], [16], [17], stroke [7], [18], epilepsy [7], [19] and tumors [7]. For example, Buckner et al. [15] were able to demonstrate a correlation between the site of the targeted regions and the location of major hubs in Alzheimer's disease. He et al. [13] have also shown different structural variation of brain small-world organization in individuals with

Alzheimer’s disease, which has been shown to accurately classify people with Alzheimer’s disease. Similarly, Liu et al. [20] have shown the network properties in individuals with schizophrenia relative to controls.

In addition to understanding dysfunctional networks in pathological conditions, the brain networks involved in affect regulation, motor control and execution, and learning and memory are important for understanding normal brain development and function. Hence, researchers have used graph theoretical approaches to examine learning-related changes in network connectivity [21]. In order to establish a brain network using modern graph theory, there are a number of steps to be taken [12], [22], [23]: (1) define the network nodes, (2) estimate association/correlation between nodes, (3) compile pairwise associations between nodes and generate an association matrix, and (4) calculate the network characteristics. All of these steps require a choice of a suitable approach in order to obtain an adequate network representation. Yet, despite this emerging literature, many researchers using graph theoretical approaches for fMRI data have not closely examined whether their data violate the assumptions of graph-theory. In particular, in order to make an informed decision regarding the analytical approach we need to first understand whether the fMRI time series are stationary, i.e., if the statistical properties such as mean and variance of a time series are time-invariant [24]. The assumption of fMRI stationarity is especially important in the second step to understand whether the choice of an analytical approach needs to be robust to non-stationarities. Furthermore, the stationarity of fMRI time series is relevant when discussing simple meaningful statistics of fMRI time series such as means, variances, and correlations. These statistics are more useful as a description of the data if the time-series is stationary [25], [26]. The stationarity is also relevant to the frequency analysis of the fMRI time series as the Fourier transform is suitable for stationary signals [27]. In this work, we used reverse arrangement analysis to quantify the degree of non-stationarity in fMRI data in the context of network connectivity. Such investigation will help us define the most appropriate approaches that should be considered in the establishment of connectivity matrices and complex brain networks.

2 Time series and stationarity

A set of observations recorded at a specific time is usually denoted as a time series [25]. If the observations are recorded continuously with time, then we say it is a continuous time series. On the other hand, if $x(n)$ denotes observations made within time interval $0 \leq n \leq N - 1$, where N represents the length of the signal, then $x(n)$ is a discrete time series since the observations are

made at time intervals from the discrete set γ . This time series can be considered as a realization of random variables $\{X_n, n \in \gamma\}$ [25]. Stationarity is either strong stationarity (strict stationarity) or weak (wide sense) stationarity. If the statistical properties of a time series are time-invariant, then this time series is said to have strict stationarity [24], i.e.:

$$F_{X_{n_1}, \dots, X_{n_k}}(x_1, x_2, \dots, x_N) = F_{X_{n_1+h}, \dots, X_{n_k+h}}(x_1, x_2, \dots, x_N) \quad (1)$$

for all positive integers h and for all $(n_1, \dots, n_k) \in \mathbb{Z}$. In other words, strict stationary time series should express similar statistical properties in the graphs of two equal-length time interval of realization [25]. A time series is considered to have weak or (wide-sense) stationarity if the only first two moments are time-invariant [26], such that the mean is constant, i.e.,

$$E(X_{n_1}) = E(X_{n_1+h}) \quad (2)$$

and the covariance only depends on the time lag between two observations [25], i.e.,

$$Cov(X_{n_1}, X_{n_2}) = Cov(X_{n_1+h}, X_{n_2+h}) \quad (3)$$

A usual first in the time series analysis is the visual inspection of the series in order potentially determine suitable analysis methods and/or statistical variables beneficial for summarizing information contained in the series [26].

To understand which mathematical approaches should be adopted, we need to understand the stationarity of the time series [28]. To examine the time series stationarity, one of the following non-parametric tests is applied: a run test, a reverse arrangement test (RAT), or a modified RAT [27]. The RAT is a non-parametric test that has often been used to evaluate the wide-sense stationarity of a time series [29], [30], especially to investigate the weak stationarity of physiological and biomedical signals [4], [30], [31], [32], [33], [34]. Basically, the RAT test is used to search for monotonic trends in the mean square values calculated within non-overlapping intervals of a particular time series signal of interest [29], [35]. In this study we performed the RAT test. Below are the steps we took to use the RAT test to examine the stationarity of the fMRI motor sequence learning task-related brain activation signal pattern.

1. A time series is divided into M equal non-overlapping segments. The number of segments M can be determined using the following equation:

$$M = \frac{N}{L} \quad (4)$$

where N is the length of the time series and L is the desired segment length.

2. Calculate the square mean value $Y(k)$ for each segment:

$$Y(k) = \frac{1}{L} \sum_{i=kL}^{(k+1)L-1} x^2(i) \text{ for } 0 \leq k \leq M-1 \quad (5)$$

3. The total number of reverse arrangements A is then counted within the sequence of mean square values Y_0, Y_1, \dots, Y_{M-1} . A reverse arrangement occurs when the square mean value of one segment is greater than the mean square values of the subsequent segment, i.e. when: $Y_a > Y_b$ for $a < b$. Hence, using this condition, Y_k will form the indicator:

$$s(k, d) = \begin{cases} 1 & \text{if } Y(k) > Y(k+d) \\ 0 & \text{otherwise} \end{cases} \quad (6)$$

For $1 < d \leq D$, where $D = M - k - 1$; and therefore, for k^{th} time step, the reverse arrangement test is given by:

$$A(k) = \sum_{d=1}^D s(k, d) \quad (7)$$

and the total number of reverse arrangement test A is given by:

$$A_T = \sum_{k=0}^{M-1} A(k) \quad (8)$$

4. The calculated value of the total reverse arrangement A_T from the previous step is then compared to the value that would be expected from a realization of a weakly stationary random process. If we considered the sample as weakly stationary, then the expected value of A has a normal distribution [29] with the mean given by:

$$\mu_T = \frac{L(L-1)}{4} \quad (9)$$

and the variance:

$$\sigma_T^2 = \frac{L(L-1)(2L+5)}{72} \quad (10)$$

The null hypothesis that Y_k is weakly stationary is rejected if the calculated A_T falls outside the critical values defined by a significance level α . In this research, the critical values were determined from the calculation of the stationarity test statistic Z_T , which is given by:

$$Z_T = \frac{A_T - \mu_T}{\sigma_T} \quad (11)$$

where $Z_T \sim N(0,1)$, and the critical values of Z_T at the significant level α can be defined as $Z_{1-\alpha/2}$ and $Z_{\alpha/2}$, where Z is a standard normal variate. At 5% significance level, the values of Z are given by $Z_{1-\alpha/2} = -1.96$ and $Z_{\alpha/2} = 1.96$; and the values of the test statistics Z_T will have one of the following possibilities:

- $Z_{\alpha/2} < Z_T < Z_{1-\alpha/2}$: the null hypothesis that the time series is wide sense or weakly stationary is accepted.
- $Z_T \geq Z_{1-\alpha/2}$: this means that the number of reverse arrangements is greater than that expected of a stationary signal. This implies an existence of downtrend in the mean square sequence.
- $Z_T \leq Z_{\alpha/2}$: this means that the number of reverse arrangements is less than that expected of a stationary signal. This implies an existence of an upward trend in the mean square sequence.

3 Methodology

3.1 Participants

Twelve (6 males and 6 females) healthy young adult participants (age range from 19 to 48 years old, mean age 33 years old) participated in this experiment approved by the Institutional Review Board at the University of Pittsburgh. A written informed consent was obtained from all participants after the nature of the experiment had been explained. All participants were right handed.

3.2 Data acquisition

Data acquisition was conducted by an expert fMRI technician from the Department of Radiology, University of Pittsburgh, Pittsburgh, PA. The MRI scanning was acquired on a 3T Siemens TRIO scanner using a 12-channel parallel receive head coil. GE-EPI BOLD (FA=90 deg; TR=2000 ms; TE=29 ms) scans were collected with thirty-eight axial slices (3.4 mm thickness) with a 3.4 mm x 3.4 mm in-plane resolution (64x64). A T2-weighted structural scan (FA=150 deg, TR=3000 ms, TE=11/101 ms) with voxel size 10.30 x 31.0 x 31.0 mm (matrix 256x224x256) was used to acquire 48 slices covering the whole brain which was collected prior to the functional scans. Head movement was minimized during the experiment by placing pillows around the head within the head coil.

Each of the 60 second blocks consisted of a series of 7 tapping sequences as shown in Figure 1.

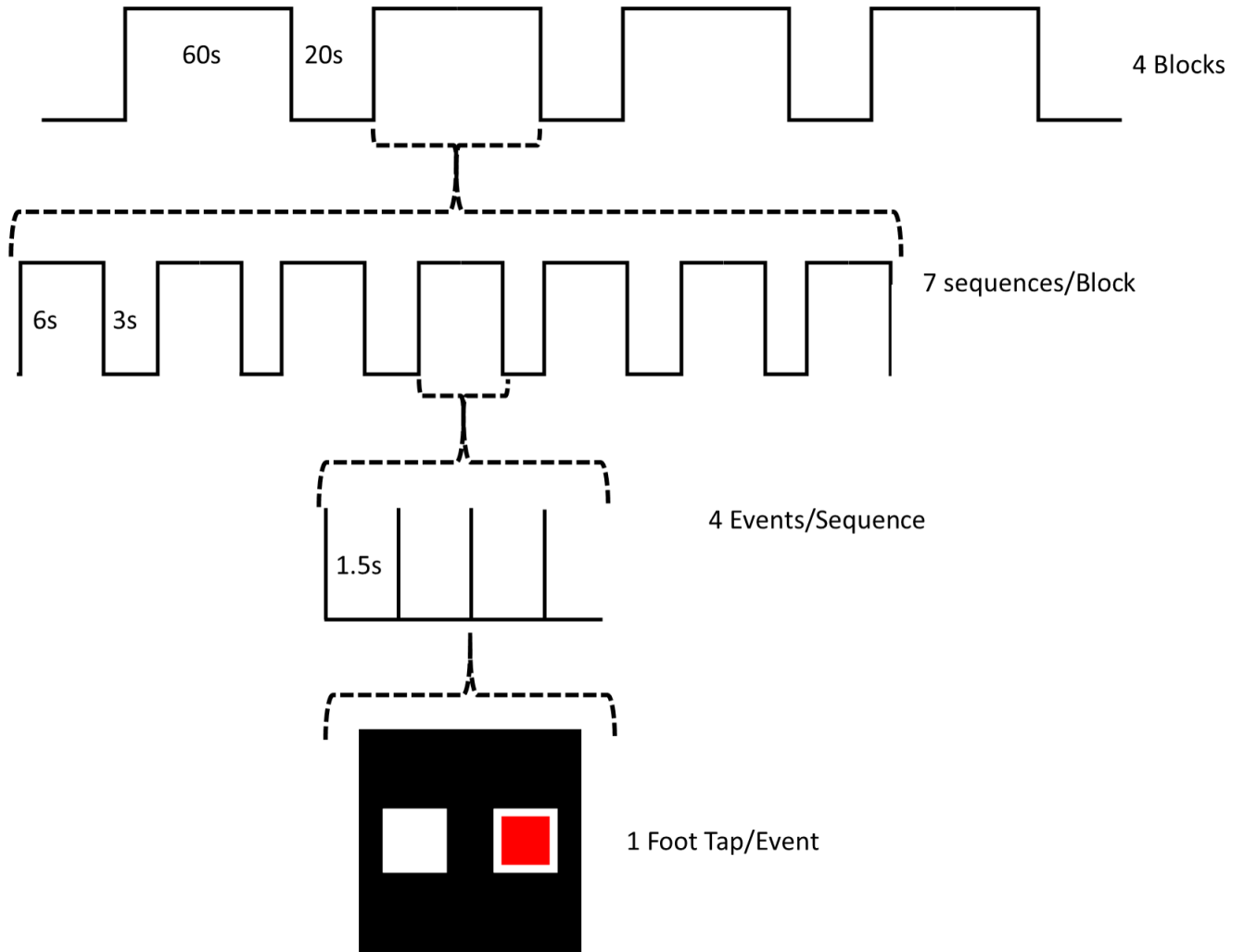


Figure 1: A flowchart depicting the fMRI protocol of the experiment.

Each sequence consisted of 4 directed movements (e.g. 7 sequences/block x 4 movements/sequence = 28 total movements/block). For the control blocks, 7 random tapping sequences were presented with no repeats. For the learning blocks, an identical tapping sequence was repeated 7 times. Each learning block used a different sequence so that each learning block required relearning the sequence. For each movement, participants were presented with a red box either on the left or right side of a display screen mounted at the head of the MR scanner, which was viewed using a mirror affixed above the head coil. Participants were told to perform ankle plantar flexion (foot tap) with either the right or left foot depending on if the box appeared on the right or left side, respectively. During the control sequence, the pattern of foot tapping was random and subjects were not expected to

learn the sequence. During the learning sequence, subjects also repeated the same sequence 7 times per 60 second block; thus they were expected to learn the pattern, as demonstrated by a decrease in foot tap onset latencies. Participants were instructed to simply perform the foot tapping task as indicated by the position of the red box projected on the screen. They were not informed that the intent was to study motor sequence learning. An overall diagram of the experimental sequence is shown in Figure 2.



(a) A diagram showing the experimental sequence in learning process.



(b) A diagram showing the experimental sequence in control process.

Figure 2: A diagram showing the experimental sequence in learning and control process.

3.3 Data preprocessing

The Statistical Parametric Mapping (SPM) toolbox was utilized to preprocess and analyze the acquired fMRI data [11]. Data preprocessing steps included: realignment or (motion correction), coregistration, normalization, and smoothing. The realignment is performed using the least square method and a six parameter spatial transformation [36]. The movement artifacts and excessive head motion in the fMRI scans was removed in this procedure using a well known approach [20]. Next, the mean functional image generated from the previous realignment step is co-registered to a high resolution anatomical image and all of the other functional images are then resliced to align with the reference image. To normalize the scans between different subjects, we utilized the standard template image in MNI space (Montreal Neurological Institute) [10]. Unlike the rigid body realignment to correct for motion, normalization includes changing the size of the brain to match the size and position of the template. Hence, smoothing is performed to: increase the signal to noise ratio, increase inter-subject overlap, and to increase the validity of the analysis. Smoothing includes blurring the functional MRI images using a Gaussian filter (i.e data is convolved with

a Gaussian kernel) [37]. After smoothing the images, each voxel becomes a weighted region of interest (ROI, the voxels under the kernel). The size of the new voxel can be obtained using the full width half maximum technique (FWHM) [3], which is an indication of the distribution of the kernel values. Ideally, the FWHM kernel size should be chosen to match the size of the expected activation

After the scans were processed and registered with the MNI template image, the scans were all segmented into 90 cortical and subcortical anatomical ROIs using the MarsBAR toolbox [38]. The mean time series for each of the 90 regions of interest (ROIs) were computed by averaging all voxels within each region at each time point in the time series, resulting in 170 data points for each of the 90 anatomical ROIs. Since the human brain has two cerebral hemispheres, the 90 regions are divided equally between the left and the right hemisphere, i.e. 45 ROIs in each hemisphere. This was done by using the Automated Anatomical Labeling template (AAL) [39]. Cerebellum regions were not included as the fMRI scans did not cover these regions.

3.4 Data Analysis

The data analysis consisted of the fMRI scans from three different runs of foot tapping sequences for each of the 12 participants. The first and the third runs were acquired while the participants performed the foot tapping sequences of the learning-control-learning-control set. The second run was acquired while the participants performed foot tapping task in the order of the control-learning-control-learning set. Using the acquired images, we extracted 90 time series of length 170 data points for each participant.

Next, we used the RAT to investigate the stationarity of the fMRI time series. At an increment of one, we tested stationarity at various window sizes (10 to 15 scans) for each time series. The window size selection is based on a window that will maintain enough data points to estimate a single statistical parameter for the calculation of both the mean squared value within each interval and the total number of reverse arrangements [35]. The null hypothesis of time invariance was then tested at 5% level of significance. For time-varying time series, we utilized a regression analysis to identify whether the time series had a varying mean and/or variance. Furthermore, we identified the mean and variance as either having an increasing or decreasing trend at the 5% significance level.

4 Results

4.1 Effects of window size

Once the 170 data points had been processed, we computed 90 fMRI time series that have been used for stationarity testing using the RAT Test. It can be clearly seen from Figure 3 (a)-(d) below that the greatest percentage of non-stationary signals were distinguished during the first and second runs of the fMRI task, while the least number of non-stationary signals were found within the last run.

The impact of a window size on stationarity is depicted in Figure 3(d). The percentage of non-stationary time series decreased with increasing window size; but this effect is not statistically significant due to a few window size increments ($p > 0.75$). At larger window sizes, a time series is divided into fewer segments and fewer comparisons between subsequent mean square values are carried out. This process will reduce the number of opportunities to detect a reverse arrangement. The boxplots on the other hand show the stationarity of the test statistics value Z_T at different window sizes for the three runs. In each of the three sub-figures, the two horizontal dashed lines represent the boundary between stationarity and non-stationarity of the data based on the value of Z_T defined by $|Z| < 1.96$.

From the boxplots in Figure 3 (a)-(c), we can observe the following:

- The fMRI time series were generally stationary since the median values of the stationary test statistic Z_T fell within the stationarity range at the 5% significance level previously defined and represented by the two dashed lines at each figure ; i.e. $|Z| < 1.96$.
- It can be also noticed from the first and last runs R1 and R3, which have the same task sequence, that only in the last run R3 the 25% and 75% of the Z_T values fell within that range. For the first run R1, only the 25 percentile fell within the range. In each run (R1,R2 and R3) as shown in Figure 3, the number of stationary time series tended to increase with increasing window size.
- With increasing window size, the variation in the stationary statistic remains relatively constant as shown in Figure 3. Therefore, an intermediate value of 13 points is utilized for further analysis.

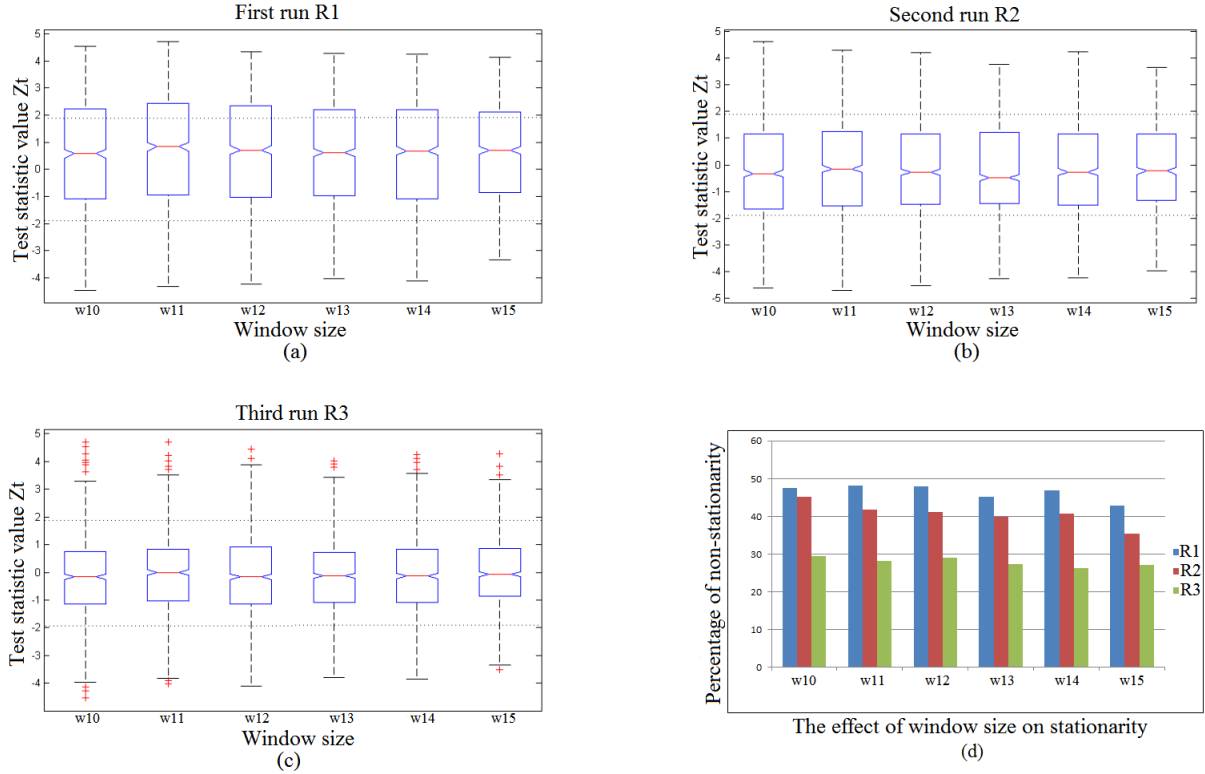


Figure 3: The effect of window size on the stationarity test statistic, Z_T , during the foot tapping task: first run R1 (a), second run R2 (b), and third run R3 (c); and the effect of window size on the percentage of non-stationary time series identified for each of the three runs (R1 = run-1, R2 = run-2, R3 = run-3) respectively (d). R1 and R3 are motor learning set runs; R2 is a control set run.

4.2 Sources of non-stationarity

As defined at the beginning of this paper a time series is said to be strictly stationary if its statistical properties are time-invariant. We investigated the sources of non-stationarity using the intermediate window size 13. It can be noticed that the last time course will be trimmed from every time series because of the indivisibility of time series lengths on the window size. We then calculated the mean and variance for each segment and tested for a significant linear regression relationship. What we observed from the extracted fMRI signals as shown in Figure 4 is that the non-stationarities can be mostly attributed to a change in the mean value over time. Furthermore, very few signals experiences time-dependant variance alone, and fewer signals demonstrated both

non-stationary means and variances.

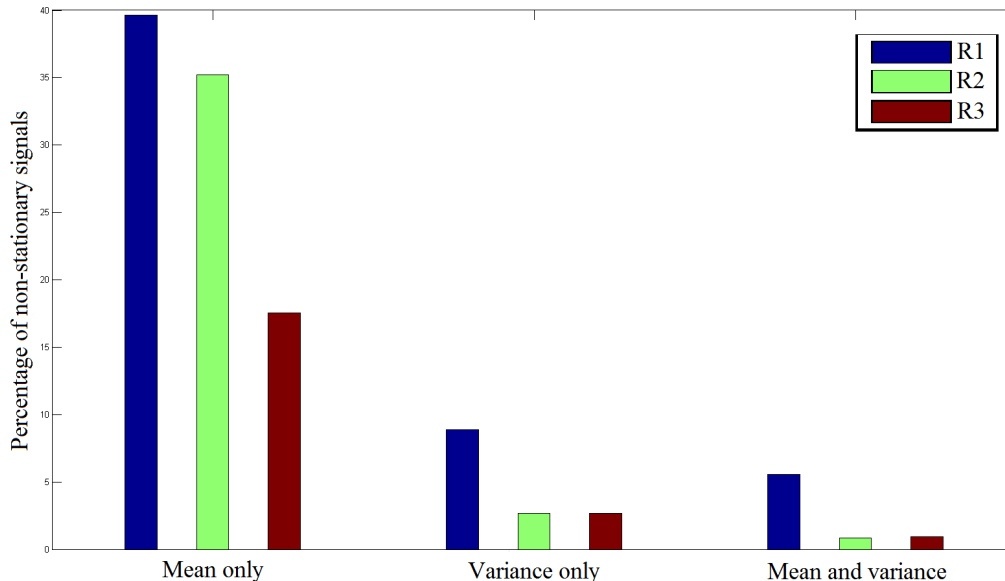


Figure 4: Sources contributing to non-stationarity time series as a percentage of non-stationary time series identified within each foot tapping task run: R1 = run 1, R2 = run 2, R3 = run 3.

Based on our observation, non-stationarity was found in different brain regions rather in specific brain regions. However, the regions that were seen stationarity among all participants are listed in Table 1.

Table 1: Stationary regions among all participants.

Region Name	Location on Hemisphere
Amygdala	left hemisphere
Caudate	left hemisphere
Caudate	right hemisphere
Medial Orbitofrontal Gyrus	left hemisphere
Insula	right hemisphere
Olfactory	left hemisphere
Inferior Parietal Gyrus	right hemisphere
Superior Parietal Gyrus	left hemisphere
Precuneus	left hemisphere
Supramarginal Gyrus	left hemisphere
Middle Temporal Gyrus	left hemisphere
Superior Temporal Pole	left hemisphere
Superior Temporal Gyrus	left hemisphere

These regions are illustrated in Figure 5. The intensity of colors in the image does not reflect the amount or the percentage of stationarity/non-stationarity but rather reflects depth of the region in the brain. So the regions that are deep in the brain have low intensities, whereas the regions that are closer to the cortex have a higher intensity.

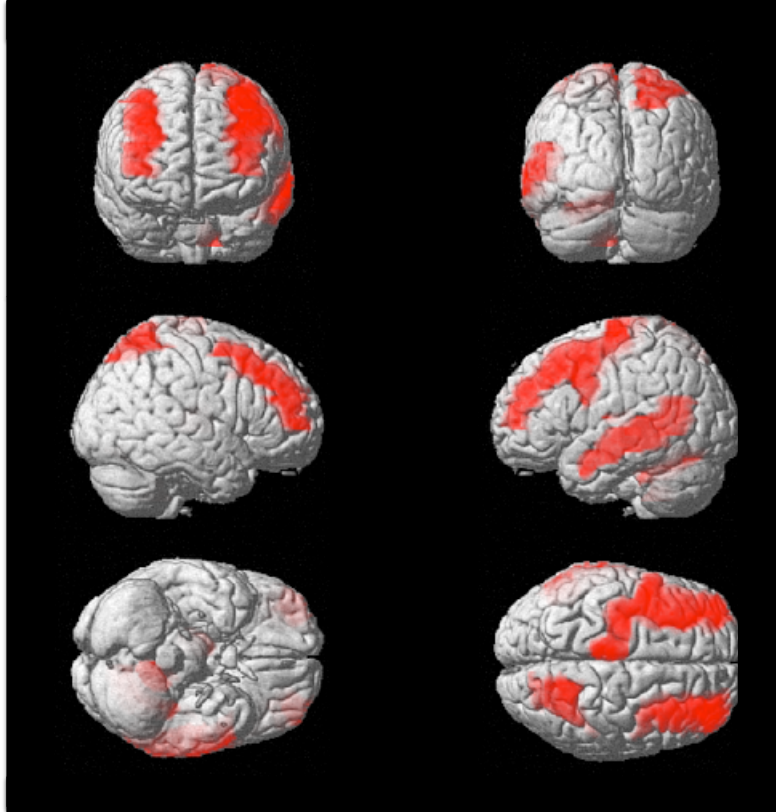


Figure 5: Brain regions found stationary in all participants. Brain images are shown in the sequence: Front-Back, Right-Left, Bottom-Top.

5 Discussion

The human brain has been viewed as one of the most complicated physiological networks [40]. Researchers try to understand how brain networks respond and interact to different stimuli using neuroimaging techniques. Our investigation informed us about the suitability of potential signal processing tools to be used to evaluate and establish the complex brain functional networks and connectivity matrices. To establish such connectivity matrices and analyze them, we need to utilize graph-theoretical approaches which have been shown to provide a powerful new way to quantify and

analyze brain structural and functional networks [12]. Such tools were initially applied to fMRI time series [41], as a way to identify functional clusters of activated brain regions during a finger tapping task. Since then, the graph theory has become a leading approach to analyze brain networks when researchers were also able to find strong and significant correlations between locally and distant (intra- and inter-hemispheric) brain regions [40]. However, one of the first steps in utilizing the graph-theoretical approaches is to compute a measure of correlation among the considered brain regions. Previous studies utilized cross-correlation [42], cross-coherence [43], and mutual information [5] among others. However, given that some fMRI time series are non-stationary, approaches resistant to non-stationarities should be considered (e.g., wavelets [44], [45], [46]).

We observed fewer non-stationarities in R3 than in R1, even-though the signal was acquired under the same stimuli and the same experimental procedure. This could be interpreted as a result of “priming” a phenomenon defined as “a change in the speed, bias or accuracy of the processing of a stimulus, following prior experience with the same, or a related, stimulus” [47]. The implicit memory phenomenon, known as direct or repetition priming, has been considered as one of the three different categories of priming [48]. From the brain activation point of view, implicit memory captures the effect of previous experience on the current experiment, even in the absence of conscious awareness of the past [47], [49], [50], [51], [52]. Moreover, repetition can also be another main reason of decreased brain activation and blood flow level in the repeated task R3. Neural activity usually decreases for repeating stimuli [53]. In particular, Gruber and Muller have discussed the repetition priming task using electroencephalogram technology [54] by analyzing the induced gamma band activity during the repetition of familiar and unfamiliar line drawings. Penhune and Doyon have also discussed such phenomenon and revealed a dynamic network of motor structures which have different activation during different phases of learning and repetition. They have shown that the recall of motor sequences in humans is mediated predominantly by cortical networks which suggest the involvement of cerebellar mechanisms in the early learning procedures. These cerebellar mechanisms are no longer recalled or involved in the repeated tasks [55].

Repetition suppression has also been observed using fMRI and PET technologies; referred to as the “response suppression phenomenon” [56] or “decremental responses” [57]. Processing a stimuli more than once will produce what is called the “sharpening phenomenon” of the stimuli’s cortical representation. This can be explained as some of the neurons that processed and coded the stimuli at the beginning will exhibit a lower response in the repeated task showing “a response suppression phenomenon.” The lower response from the previous neurons decreases the mean firing rate of a neuron population resulting in a decrease in the captured fMRI signal [47].

6 Conclusion

In this paper, we have successfully investigated the stationarity of fMRI time series in 12 healthy participants while they performed motor sequence learning foot tapping tasks in three different runs. We found that stationarity and non-stationarity were not concentrated or found in specific brain regions so that further analysis and interpretation can be introduced. We showed that some of the extracted time series are non-stationary, primarily in the form of time-varying mean. The finding reported in this study provide a new insight into what approach should be considered prior to establishing the connectivity matrices. Our results have implications for future studies as researchers should utilize techniques robust for non-stationarities.

Acknowledgment

This work was supported in part by the Pittsburgh Claude D. Pepper Older Americans Independence Center (NIA P30 AG 024827). We would also like to thank the Pittsburgh Claude D. Pepper Older Americans Independence Center Neuroimaging Working Group for development of the MR compatible force platform.

References

- [1] A. M. Dale and E. Halgren, “Spatiotemporal mapping of brain activity by integration of multiple imaging modalities,” *Current Opinion in Neurobiology*, vol. 11, no. 2, pp. 202–208, 2001.
- [2] S. M. Smith, M. Jenkinson, M. W. Woolrich, C. F. Beckmann, T. E. Behrens, H. Johansen-Berg, P. R. Bannister, M. De Luca, I. Drobnjak, D. E. Flitney *et al.*, “Advances in functional and structural MR image analysis and implementation as FSL,” *Neuroimage*, vol. 23, pp. S208–S219, 2004.
- [3] K. J. Friston, A. Holmes, J.-B. Poline, C. J. Price, and C. Frith, “Detecting activations in PET and fMRI: Levels of inference and power,” *Neuroimage*, vol. 4, no. 3, pp. 223–235, 1996.
- [4] M. Bilodeau, M. Cincera, A. B. Arsenault, and D. Gravel, “Normality and stationarity of EMG signals of elbow flexor muscles during ramp and step isometric contractions,” *Journal of Electromyography and Kinesiology*, vol. 7, no. 2, pp. 87–96, 1997.

- [5] J. Jeong, J. C. Gore, and B. S. Peterson, “Mutual information analysis of the EEG in patients with Alzheimer’s disease,” *Clinical Neurophysiology*, vol. 112, no. 5, pp. 827–835, May 2001.
- [6] D. Le Bihan, “Looking into the functional architecture of the brain with diffusion MRI,” *Nature Reviews Neuroscience*, vol. 4, no. 6, pp. 469–480, 2003.
- [7] M. Guye, G. Bettus, F. Bartolomei, and P. J. Cozzone, “Graph theoretical analysis of structural and functional connectivity MRI in normal and pathological brain networks,” *Magnetic Resonance Materials in Physics, Biology and Medicine*, vol. 23, no. 5-6, pp. 409–421, 2010.
- [8] A. M. Dale, A. K. Liu, B. R. Fischl, R. L. Buckner, J. W. Beldic, J. D. Lewine, and E. Halgren, “Dynamic statistical parametric mapping: combining fMRI and EMG for high-resolution imaging of cortical activity,” *Neuron*, vol. 26, no. 1, pp. 55–67, 2000.
- [9] S. Ogawa, T. Lee, A. Kay, and D. Tank, “Brain magnetic resonance imaging with contrast dependent on blood oxygenation,” *Proceedings of the National Academy of Sciences*, vol. 87, no. 24, pp. 9868–9872, 1990.
- [10] M. Vink, M. Raemaekers, A. van der Schaaf, R. Mandl, and N. Ramsey, “Pre-processing and analysis,” 2007.
- [11] R. A. Poldrack, J. A. Mumford, and T. E. Nichols, *Handbook of Functional MRI Data Analysis*. Cambridge University Press, 2011.
- [12] E. Bullmore and O. Sporns, “Complex brain networks: graph theoretical analysis of structural and functional systems,” *Nature Reviews Neuroscience*, vol. 10, no. 3, pp. 186–198, 2009.
- [13] Y. He, Z. Chen, and A. Evans, “Structural insights into aberrant topological patterns of large-scale cortical networks in Alzheimer’s disease,” *The Journal of Neuroscience*, vol. 28, no. 18, pp. 4756–4766, 2008.
- [14] C. Hu, L. Cheng, J. Sepulcre, G. Fakhri, Y. M. Lu, and Q. Li, “A graph theoretical regression model for brain connectivity learning of Alzheimer’s disease,” in *Int. Symp. on Biomedical Imaging*, 2013.
- [15] R. L. Buckner, J. Sepulcre, T. Talukdar, F. M. Krienen, H. Liu, T. Hedden, J. R. Andrews-Hanna, R. A. Sperling, and K. A. Johnson, “Cortical hubs revealed by intrinsic functional connectivity: mapping, assessment of stability, and relation to Alzheimer’s disease,” *The Journal of Neuroscience*, vol. 29, no. 6, pp. 1860–1873, 2009.

- [16] M.-E. Lynall, D. S. Bassett, R. Kerwin, P. J. McKenna, M. Kitzbichler, U. Muller, and E. Bullmore, “Functional connectivity and brain networks in schizophrenia,” *The Journal of Neuroscience*, vol. 30, no. 28, pp. 9477–9487, 2010.
- [17] M. P. van den Heuvel, R. C. Mandl, C. J. Stam, R. S. Kahn, and H. E. H. Pol, “Aberrant frontal and temporal complex network structure in schizophrenia: a graph theoretical analysis,” *The Journal of Neuroscience*, vol. 30, no. 47, pp. 15 915–15 926, 2010.
- [18] B. J. He, A. Z. Snyder, J. L. Vincent, A. Epstein, G. L. Shulman, and M. Corbetta, “Breakdown of functional connectivity in frontoparietal networks underlies behavioral deficits in spatial neglect,” *Neuron*, vol. 53, no. 6, pp. 905–918, 2007.
- [19] M. Vlooswijk, M. Vaessen, J. Jansen, M. de Krom, H. Majoie, P. Hofman, A. Aldenkamp, and W. Backes, “Loss of network efficiency associated with cognitive decline in chronic epilepsy,” *Neurology*, vol. 77, no. 10, pp. 938–944, 2011.
- [20] Y. Liu, M. Liang, Y. Zhou, Y. He, Y. Hao, M. Song, C. Yu, H. Liu, Z. Liu, and T. Jiang, “Disrupted small-world networks in schizophrenia,” *Brain*, vol. 131, no. 4, pp. 945–961, 2008.
- [21] S. Sami and R. C. Miall, “Graph network analysis of immediate motor-learning induced changes in resting state BOLD,” *Frontiers in Human Neuroscience*, vol. 7, 2013.
- [22] M. Rubinov and O. Sporns, “Complex network measures of brain connectivity: Uses and interpretations,” *Neuroimage*, vol. 52, no. 3, pp. 1059–1069, 2010.
- [23] J. C. Reijneveld, S. C. Ponten, H. W. Berendse, and C. J. Stam, “The application of graph theoretical analysis to complex networks in the brain,” *Clinical Neurophysiology*, vol. 118, no. 11, pp. 2317–2331, 2007.
- [24] C. Chatfield, *The analysis of time series: an introduction*. Chapman and Hall/CRC, 2003, vol. 59.
- [25] P. J. Brockwell and R. A. Davis, *Time series: theory and methods*. Springer, 2009.
- [26] R. H. Shumway and D. S. Stoffer, *Time Series Analysis and its Applications*. Springer Science+ Business Media, 2010.
- [27] T. W. Beck, T. J. Housh, J. P. Weir, J. T. Cramer, V. Vardaxis, G. O. Johnson, J. W. Coburn, M. H. Malek, and M. Mielke, “An examination of the runs test, reverse arrangements test, and

- modified reverse arrangements test for assessing surface EMG signal stationarity,” *Journal of Neuroscience Methods*, vol. 156, no. 1, pp. 242–248, 2006.
- [28] R. Manuca and R. Savit, “Stationarity and nonstationarity in time series analysis,” *Physica D: Nonlinear Phenomena*, vol. 99, no. 2, pp. 134–161, 1996.
- [29] J. S. Bendat and A. G. Piersol, “Random data analysis and measurement procedures,” *Measurement Science and Technology*, vol. 11, no. 12, p. 1825, 2000.
- [30] N. Alves and T. Chau, “Stationarity distributions of mechanomyogram signals from isometric contractions of extrinsic hand muscles during functional grasping,” *Journal of Electromyography and Kinesiology*, vol. 18, no. 3, pp. 509–515, 2008.
- [31] K. M. Hampson, I. Munro, C. Paterson, and C. Dainty, “Weak correlation between the aberration dynamics of the human eye and the cardiopulmonary system,” *Journal of the Optical Society of America A*, vol. 22, no. 7, pp. 1241–1250, 2005.
- [32] G. F. Harris, S. A. Riedel, D. Matesi, and P. Smith, “Standing postural stability assessment and signal stationarity in children with cerebral palsy,” *IEEE Transactions on Rehabilitation Engineering*, vol. 1, no. 1, pp. 35–42, 1993.
- [33] B. Nhan and T. Chau, “Infrared thermal imaging as a physiological access pathway: A study of the baseline characteristics of facial skin temperatures,” *Physiological Measurement*, vol. 30, no. 4, p. N23, 2009.
- [34] V. Novak, G. Honos, and R. Schondorf, “Is the heart empty at syncope?” *Journal of the Autonomic Nervous System*, vol. 60, no. 1, pp. 83–92, 1996.
- [35] T. Chau, D. Chau, M. Casas, G. Berall, and D. J. Kenny, “Investigating the stationarity of paediatric aspiration signals,” *IEEE Transactions on Neural Systems and Rehabilitation Engineering*, vol. 13, no. 1, pp. 99–105, 2005.
- [36] L. Freire, A. Roche, and J.-F. Mangin, “What is the best similarity measure for motion correction in fMRI time series?” *IEEE Transactions on Medical Imaging*, vol. 21, no. 5, pp. 470–484, 2002.
- [37] T. S. Braver, J. D. Cohen, L. E. Nystrom, J. Jonides, E. E. Smith, and D. C. Noll, “A parametric study of prefrontal cortex involvement in human working memory,” *Neuroimage*, vol. 5, no. 1, pp. 49–62, 1997.

- [38] M. Brett, J.-L. Anton, R. Valabregue, and J.-B. Poline, “Region of interest analysis using the marsbar toolbox for SPM 99,” *Neuroimage*, vol. 16, p. S497, 2002.
- [39] N. Tzourio-Mazoyer, B. Landeau, D. Papathanassiou, F. Crivello, O. Etard, N. Delcroix, B. Mazoyer, M. Joliot *et al.*, “Automated anatomical labeling of activations in SPM using a macroscopic anatomical parcellation of the MNI MRI single-subject brain,” *Neuroimage*, vol. 15, no. 1, pp. 273–289, 2002.
- [40] C. J. Stam and J. C. Reijneveld, “Graph theoretical analysis of complex networks in the brain,” *Nonlinear Biomedical Physics*, vol. 1, no. 1, p. 3, 2007.
- [41] S. Dodel, J. M. Herrmann, and T. Geisel, “Functional connectivity by cross-correlation clustering,” *Neurocomputing*, vol. 44, pp. 1065–1070, 2002.
- [42] G. J. Siegle, W. Thompson, C. S. Carter, S. R. Steinhauer, and M. E. Thase, “Increased amygdala and decreased dorsolateral prefrontal BOLD responses in unipolar depression: Related and independent features,” *Biological Psychiatry*, vol. 61, no. 2, pp. 198–209, Jan. 2007.
- [43] F. T. Sun, L. M. Miller, and M. D’Esposito, “Measuring interregional functional connectivity using coherence and partial coherence analyses of fMRI data,” *NeuroImage*, vol. 21, no. 2, pp. 647–658, Feb. 2004.
- [44] E. Bullmore, J. Fadili, V. Maxim, L. Şendur, B. Whitcer, J. Suckling, M. Brammer, and M. Breakspear, “Wavelets and functional magnetic resonance imaging of the human brain,” *Neuroimage*, vol. 23, pp. S234–S249, 2004.
- [45] I. Daubechies, “The wavelet transform, time-frequency localization and signal analysis,” *IEEE Transactions on Information Theory*, vol. 36, no. 5, pp. 961–1005, 1990.
- [46] S. Achard and E. Bullmore, “Efficiency and cost of economical brain functional networks,” *PLoS Computational Biology*, vol. 3, no. 2, p. e17, 2007.
- [47] R. Henson, “Neuroimaging studies of priming,” *Progress in Neurobiology*, vol. 70, no. 1, pp. 53–81, 2003.
- [48] D. L. Schacter, “Priming and multiple memory systems: Perceptual mechanisms of implicit memory,” *Journal of Cognitive Neuroscience*, vol. 4, no. 3, pp. 244–256, 1992.

- [49] P. Graf, L. R. Squire, and G. Mandler, “The information that amnesic patients do not forget.” *Journal of Experimental Psychology: Learning, Memory, and Cognition*, vol. 10, no. 1, p. 164, 1984.
- [50] B. Milner, S. Corkin, and H.-L. Teuber, “Further analysis of the hippocampal amnesic syndrome: 14-year follow-up study of HM,” *Neuropsychologia*, vol. 6, no. 3, pp. 215–234, 1968.
- [51] B. Hauptmann and A. Karni, “From primed to learn: the saturation of repetition priming and the induction of long-term memory,” *Cognitive Brain Research*, vol. 13, no. 3, pp. 313–322, 2002.
- [52] E. K. Warrington and L. Weiskrantz, “The effect of prior learning on subsequent retention in amnesic patients,” *Neuropsychologia*, vol. 12, no. 4, pp. 419–428, 1974.
- [53] K. Grill-Spector, R. Henson, and A. Martin, “Repetition and the brain: neural models of stimulus-specific effects,” *Trends in Cognitive Sciences*, vol. 10, no. 1, pp. 14–23, 2006.
- [54] T. Gruber and M. M. Müller, “Oscillatory brain activity dissociates between associative stimulus content in a repetition priming task in the human EEG,” *Cerebral Cortex*, vol. 15, no. 1, pp. 109–116, 2005.
- [55] V. B. Penhune and J. Doyon, “Dynamic cortical and subcortical networks in learning and delayed recall of timed motor sequences,” *The Journal of Neuroscience*, vol. 22, no. 4, pp. 1397–1406, 2002.
- [56] R. Desimone, “Neural mechanisms for visual memory and their role in attention,” *Proceedings of the National Academy of Sciences*, vol. 93, no. 24, pp. 13 494–13 499, 1996.
- [57] M. Brown and J.-Z. Xiang, “Recognition memory: Neuronal substrates of the judgement of prior occurrence,” *Progress In Neurobiology*, vol. 55, no. 2, pp. 149–189, 1998.